Article:

Li, A., Li, S., Huang, S.-S. orcid.org/0000-0003-2816-7104 et al. (1 more author) (2024) Thermal creep strain test and model of Q460GJ steel at elevated temperatures. Journal of Constructional Steel Research, 223. 109082. ISSN 0143-974X

https://doi.org/10.1016/j.jcsr.2024.109082

Thermal creep strain test and model of Q460GJ steel at elevated temperatures

*Aibing Li [a], Siqi Li [a], Shan-Shan Huang [b], Weiyong Wang[a, c] **

a School of Civil Engineering, Chongqing University, Chongqing 400045, P. R. China

b Department of Civil and Structural Engineering, The University of Sheffield, Sir Frederick Mappin Building, Mappin Street, Sheffield S1 3JD, UK

c Key Laboratory of New Technology for Construction of Cities in Mountain Area (Ministry of Education), Chongqing University, Chongqing 400045, P. R. China

Abstract: Q460GJ steel is a typical high strength and high-performance structural steel. The thermal creep test on two thicknesses (8 mm and 12 mm) of Q460GJ steel plates at elevated temperatures (400-800 °C) was carried out. The test results showed that the thermal creep strain increases with the increases of temperature and stress. When the temperature exceeds about 500 °C and the stress ratio is greater than about 0.55, the Q460GJ steel plate specimens has obvious creep deformations, so it is necessary to consider the thermal creep deformation of steel at elevated temperatures for steel structural design. The difference in plate thickness does not affect the creep properties of the 8 mm and 12 mm Q460GJ steel plates at elevated temperatures. When the temperature is no more than 600 °C, the second stage creep strain rates of Q460 steel are obviously higher than that of Q460GJ steel while the stress levels are close. The Fields & Fields creep model is suitable for fitting the thermal creep strain-time curves for Q460GJ steel. The findings will contribute to providing theoretical support for design of high-performance steel engineering structures under fire.

Keywords: Q460GJ steel; At elevated temperature; Creep strain; Creep strain rate; Creep model

* Corresponding Author: W. Wang, Ph.D. & Professor, E-mail: wywang@cqu.edu.cn

1. Introduction

The research and use of steel in building structures have been developing rapidly around the world. High-strength structural steel with yield strength standard value higher than 460MPa has been more and more applied [1-2]. High-strength steel has excellent mechanical properties and economic advantages. With the continuous improvement of steel manufacture process, through the precise control of trace elements in the steel, the strength, yield to strength ratio, ductility and other properties of structural steel are gradually improved [3-4]. For example, in 2023, Chinese standard "Steel Plate for Building Structure" (GB/T 19879) [5] was updated to standardize the production and application of high-performance steel, by adding 'GJ' after the original steel grade, such as Q345GJ, commonly known as 'GJ steel'. Q460GJ steel is a typical high strength and high-performance structural steel and has been used in structures in recent ten years.

Creep refers to the phenomenon that the plastic strain of steel increases slowly with time under the action of constant and continuous stress at a certain temperature. The strength degradation of steel at high temperature is serious, and the creep strain at high temperature is much higher than that at room temperature, and the creep deformation will also increase sharply [6-8]. At the same time, current research has found that thermal creep has a great impact on the fire response of steel structural members [9-10]. The typical thermal creep curve of steel is mainly divided into three stages, namely, the instantaneous creep stage (the creep strain rate is high, but the rate gradually decreases with time), the steady-state creep stage (when the creep rate reaches the lowest value, it starts to remain constant, and then enters the steady-state creep stage) and the accelerated creep stage (with the increase of creep deformation, tiny cracks are generated between crystals, the creep rate gradually increases, and enters the accelerated creep stage). Finally, the steel fractures. In general, when the temperature is higher than 30% - 40% of the melting point of steel, obvious creep phenomenon will occur [11]. Ignoring the influence of thermal creep in structural calculation will lead to the result is not conservative, which will cause potential safety hazards.

The thermal creep behaviors of different types of steels are significantly different due to different material compositions and manufacture processes [12-14]. Wang et al. [15] found that the thermal creep of Q355 cold formed steel was more sensitive. Brnic et al. [16] conducted an experimental study on the short-time creep behavior of S355 structural steel and found it does not have creep resistance at high temperatures above 500 ºC. Wang et al. [17-18] conducted thermal creep test on high-strength steel and found that the total creep strain increased with the increase of temperature in the range of 450~600 ºC. In the temperature range of 700~900 ºC, the total creep strain was more than 45%, which was higher than the total creep strain at lower temperature. Li et al. [19] showed that under high temperature and high stress levels, the total amount of creep deformation of high-strength steel was large and the creep strain rate increased rapidly. Based on the current research review, many studies have shown that steel type, stress level and a wide range of temperature values have important effects on the creep response of structural steel [20-23]. For the simulation and theoretical calculation of steel structures at high temperature, many studies do not consider the influence of thermal creep [24-27]. The mechanical properties of high-performance steel at high temperature are very different from those of high-strength steel, especially with better ductility at high temperature [28]. This may lead to a great difference from the high temperature creep of high-strength steel. However, at present, there are few studies on the creep properties of high-performance steel, and there is no comparative analysis with the thermal creep properties of high-performance steel, such as Q460GJ steel. There is no suitable creep model to describe the thermal creep behavior of high-performance steel. In conclusion, it is necessary to carry out a comprehensive study on the thermal creep behavior of high-performance steel.

In this paper, the creep properties of Q460GJ steel at elevated temperatures were studied, and the thermal creep strain-time curves at different temperatures and stress levels were obtained, and the thermal creep strain-time curves of Q460GJ steel were compared with that of Q460 steel and analyzed. The Fields & Fields model was selected to fit the thermal creep strain-time curves of Q460GJ steel at elevated temperatures, and the creep characteristics of Q460GJ steel at elevated temperatures were comprehensively characterized. The findings will contribute to providing theoretical support for design of high-performance steel engineering structures under fire.

2. Mechanical properties of Q460GJ at elevated temperatures

Mechanical properties of high-performance steel named Q460GJ steel and high-strength steel named Q460 steel at elevated temperatures were cited from the relevant references [29-30] for comparison analyses and to design the following thermal creep tests. Two thickness of Q460GJ steel plates were adopted (8mm thickness and 12 mm thickness), which were provided by HBIS Group Co., Ltd., P. R. China manufactured in accordance with Chinese standard GB/T 19879-2023 (Steel Plate for Building Structure) [5]. The mechanical properties of Q460GJ and Q460 steel at elevated temperatures are shown in Table 1. It can be concluded that the yield strength of 8 mm thickness Q460GJ steel plate (Q460GJ-8 mm) at elevated temperatures are almost the same with that of 12 mm thickness Q460GJ steel plate (Q460GJ-12 mm) at relevant elevated temperatures. The effect of plate thickness on the mechanical properties of Q460GJ steel can be ignored. Compared with the room temperature and elevated temperatures yield strength of Q460GJ steel, it can be found that the yield strength of Q460 steel were slightly higher.

Figure 1 shows the reduction factors of Q460GJ steels [29] and Q460 steel [30] at elevated temperatures. By comparing the elastic modulus reduction factors at elevated temperatures, it is found that the elastic modulus reduction factors of Q460GJ steels steel were slightly higher than that of Q460 steel before 400 ºC, and were lower than that of Q460 steel after 400 ºC. By comparing the yield strength reduction factors at elevated temperatures, it is found that the yield strength reduction factors of Q460 steel were higher than that of Q460GJ steel. As shown in Figure 1 (c), it is found that ultimate strength reduction factors of Q460 steel were almost the same as that of Q460GJ steel.

Table 1 The yield strength (MPa) of Q460GJ and Q460 steel at elevated temperatures.

Steels	20 °C	300 °C	400 °C	500 °C	600 °C	700 °C	800 °C
Q460GJ-8 mm [29]	475	411	375	311	220	108	53
Q460GJ-12 mm [29]	495	443	415	365	249	120	54
Q460 [30]	503	575	518	430	367	182	89

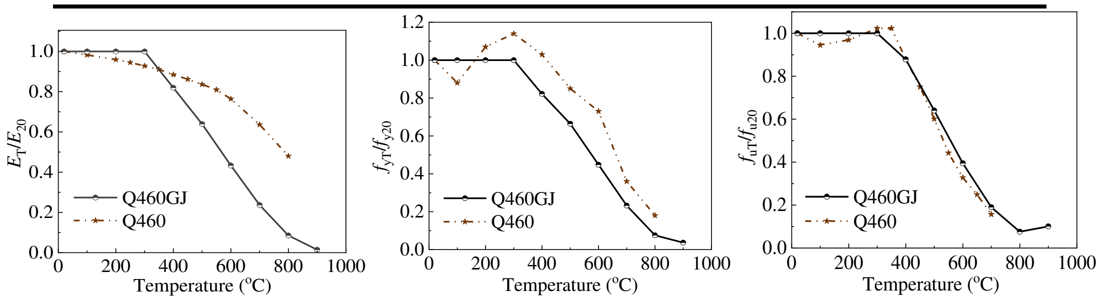

(a) Elastic modulus (b) Yield strength (c) Tension strength

Fig. 1. The reduction factors of Q460GJ [29] and Q460 steel [30].

3. Thermal creep tests for Q460GJ steels

3.1 Materials and specimen

The chemical compositions of Q460GJ steel and Q460 steel are shown in Table 2. Alloy element content determines the microstructure and macroscopic mechanical properties of steel material. The lower content of sulfur (S) and phosphorus (P) elements will be beneficial for improving the ductility and toughness of high-strength steel. Adding of Chromium (Cr), Nickel (Ni) and Molybdenum (Mo) can improve the strength of steel by improving the hardenability. Adding of vanadium (V) and aluminum (Al) can improve the strength and fracture toughness by refining the crystal structure of steel [31]. On the whole, the sulfur content is less than 0.015%, the phosphorus content is less than 0.025%, the carbon content is less than 0.20%. Sulfur and phosphorus can increase the strength and hardness of steel, but significantly decrease ductility and toughness, and increase brittleness. Commonly, these changes in chemical composition have a significant impact on mechanical properties, but less impact on anticorrosion properties.

Table 2 Chemical compositions of Q460GJ steel and Q460 steel.

Steel	Element (%)													
	C	Si	Mn	P	S	Al	Cr	Ni	Cu	Mo	Nb	V	Ti	CEV
Q460GJ	0.150	0.320	1.540	0.010	0.0008	0.039	0.050	0.020	0.030	0.004	0.034	0.037	0.003	0.420
Q460[30]	0.070	0.130	0.920	0.012	0.0030	-	-	0.020	-	-	-	-	0.064	0.246

Specimen preparation process meets the requirements of the standards GB/T 2039-2012 (ISO 204: 2023) [32] and GB/T228.2-2015 (ISO 6892-2:2011) [33]. The size of the specimen may have an impact on the results of high-temperature creep tests. Currently, due to the limitations of experimental instruments, the effect of specimen size has not been considered in this article. Figure 2 is the dimensions and actual photo of test specimen. Studs are designed in the middle of the test specimen to be used to fix the extensometer in the test, so the longitudinal distance between the studs is the gauge length. A hole with a diameter of 8 mm is designed at 22 mm from the end of the test specimen. In the test, the test specimen is fixed on the creep measurement with bolts, and the axial tension is applied to the test specimen. In the process of making the test specimen, it is necessary to ensure that the hole position is located on the longitudinal axis of the test piece, otherwise the stress distribution will be not uniform in the test, which will greatly affect the test results. The thermal creep test specimen is cut by Wire cut Electrical Discharge Machining (WEDM), and the accuracy of this cutting method can reach 0.01 mm.

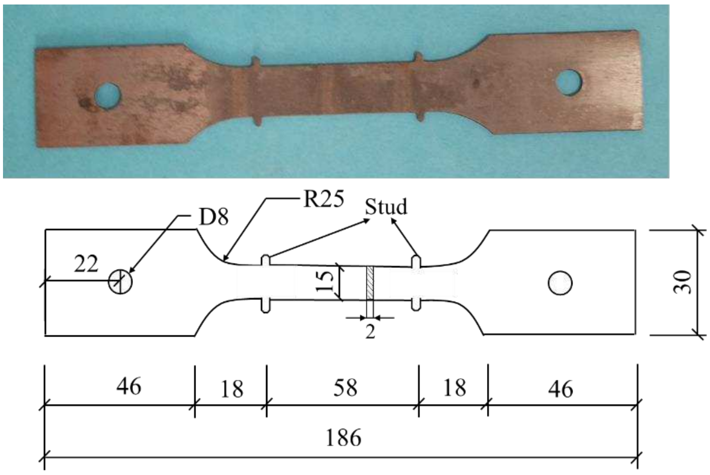

Fig. 2. Dimensions and actual photo of test specimen (mm).

Usually, the creep phenomenon of steel at low temperatures is not significant. Carbon steel with exceeding 300 °C heating and alloy steel with exceeding 400 °C heating will exhibit significant creep effects. The target elevated temperatures were selected as 400 °C, 500 °C, 600 °C, 700 °C and 800 °C, respectively. At each temperature, three tests considering different stress ratios (R) were conducted. Stress ratio was defined as the ratio of the pre-selected stress (σ) to the yield stress at elevated temperature ($f_{y,T}$). Four stress ratios were designed (0.2, 0.3, 0.55, 0.8). The numbers of test specimens and corresponding test conditions are shown in Table 3. For example, the specimen number 'GJ-8-600-0.3-1' represents 'Q460GJ steel - 8mm thickness plate - 600 °C - Stress ratio 0.3 - specimen 1'. Commonly, due to the relatively larger creep deformation values and good repeatability of thermal creep test [15], one single specimen was used for each test. Especially, for S-8-600R, S-8-700R, S-8-800R tests, two specimens were tested for checking the validity of test results.

3.2 Thermal creep test setup and process

The thermal creep test was carried out using the GMT-D100 electronic high temperature creep measurement (Figure 3), which includes a temperature control module, a strain measurement module and a loading module. GB/T 2039-2012 [32] The N-type thermocouple was directly bound to the specimen to measure the temperature within the standard distance of the specimen and at the same time automatic temperature control was carried out, three-stage temperature control was designed. The three thermocouples were respectively installed in the upper, middle and lower areas of the specimen gauge length, and the temperature control accuracy is ± 1 ºC. The heating processes at different elevated temperatures are shown in Figure 4. The heating rate of the thermoelectric furnace was 10 ºC /min, and the specimen was heated to the designed temperature without load and then kept for 30 minutes. The creep strain of the specimen was measured after loading for eliminating the effect of thermal expansion strain.

Table 3 Numbers of test specimens and corresponding test conditions.

Test number	T (ºC)	$f_{y,T}$ (MPa)	Pre-selected stress σ (MPa)	Stress ratio R (Failure mode)
GJ-8-400	400	375.82	112.7/206.7/300.7	0.3(N)/0.55(N)/0.8(N)
GJ-8-500	500	311.94	93.6/171.6/249.5	0.3(N)/0.55(N)/0.8(N)
GJ-8-600	600	220.42	66.1/121.2/176.3	0.3(N)/0.55(N)/0.8(F)
GJ-8-700	700	108.74	21.7/32.6/59.8	0.2(N)/0.3(N)/0.55(F)
GJ-8-800	800	53.78	10.7/16.1/29.6	0.2(N)/0.3(N)/0.55(F)
GJ-12-400	400	415.55	124.5/228.25/332.4	0.3(N)/0.55(N)/0.8(N)
GJ-12-500	500	365.29	109.6/200.9/292.2	0.3(N)/0.55(N)/0.8(N)
GJ-12-600	600	249.76	74.9/137.4/199.8	0.3(N)/0.55(N)/0.8(F)
GJ-12-700	700	120.18	24.0/36.1/66.1	0.2(N)/0.3(N)/0.55(F)
GJ-12-800	800	54.44	10.9/16.3/29.9	0.2(N)/0.3(N)/0.55(F)

Note: F-fracture mode; N-without fracture mode.

When the specimen installation was completed, tension load was added to the specimen with a loading rate of 500 N/s until the target load was achieved. The loading rate of 500 N/s was used to ensure that the creep strain during loading could be minimized. After loading to the target load, the load and temperature were kept constant until the specimen fractured or the loading time exceeded 6h.

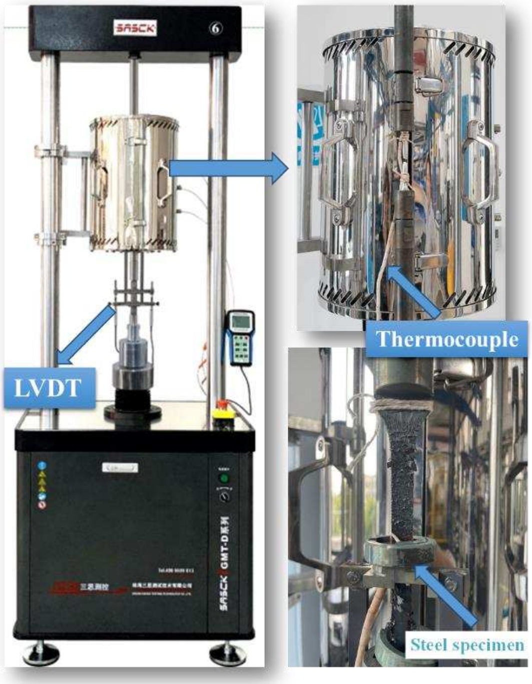

Fig. 3. Tensile testing setup and measurement.

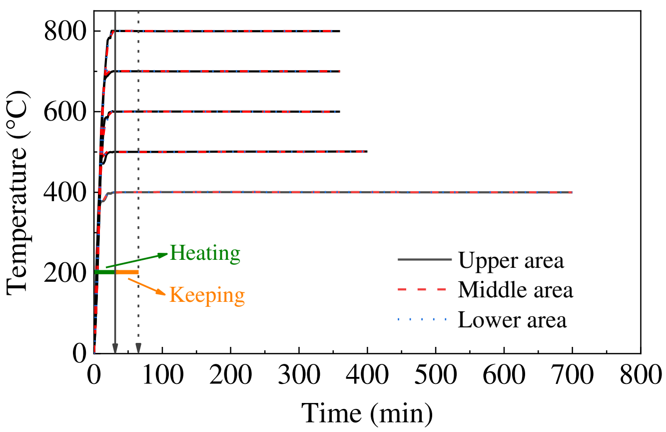

Fig. 4. Heating process for tensile testing.

4. Thermal creep test results and discussions

4.1 Failure modes of the specimen

Typical specimen photos after thermal creep test are shown in Figure 5. At 400 ºC, the surface of S-8-400R test specimen was almost intact and had metallic luster. At 500 ºC, part of the surface of S-8-500R test specimen was carbonized showing grayish black and the metallic luster faded. At 600 ºC, 700 ºC and 800 ºC, the surfaces of S-8-600R, S-8-700R, S-8-800R were black and the metallic luster faded. At 400 ºC and 500 ºC, the creep deformation amounts of the S-8-400R and S-8-500R specimens were very small and there were no necking phenomena observed. At 600 ºC, when the stress ratios were 0.3 and 0.55, the creep amounts of the S-8-600R test specimens were relatively small. But when the stress ratios were 0.8, the creep amount of the tested specimen was obvious, and the necking phenomenon occurred, and finally fracture occurred. At 700 ºC and 800 ºC, when the stress ratios were 0.2 and 0.3, the creep amounts of the S-8-700R and S-8-800R specimens were relatively small. But when the stress ratios were 0.55, the creep amount of the tested specimen was obvious, and the necking phenomenon occurred, and finally fracture occurred.

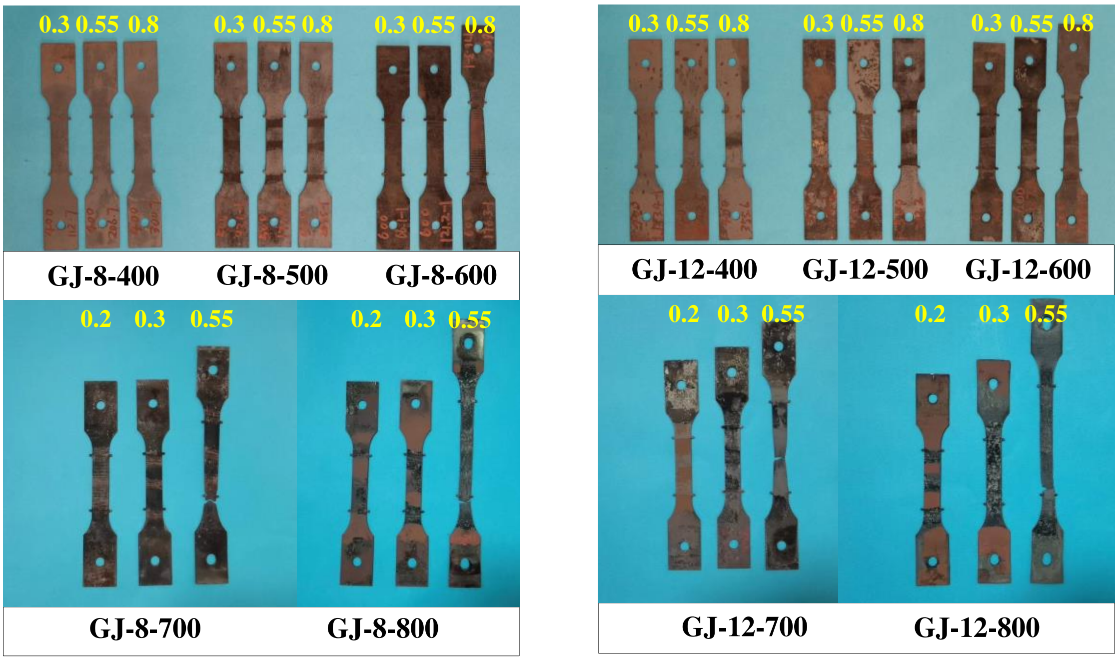

Fig. 5. Typical specimen photos after thermal creep test.

To sum up, when the temperature exceeds about 500 °C and the stress ratio is greater than about 0.55, the 8 mm thickness Q460GJ steel plate specimens has obvious creep deformations, so it is necessary to consider the creep deformation of steel at elevated temperatures for steel structural design.

For 12 mm thickness Q460GJ steel plate specimens, the failure modes observed from creep tests are almost the same with that of 8 mm thickness Q460GJ steel plate specimens. It can be concluded that the thickness effect could be negligible for Q460GJ steel plates with thicknesses of 8 mm and 12 mm.

4.2 Thermal creep strain–time curves

Thermal creep strain-time curves of Q460GJ steel specimens at different temperatures are shown in Figure 6. As shown in Figure 6 (a) and (c), the thermal creep strain-time curves only showed the first and second creep stages, which shows that the creep rate changed from fast to slow, and then tended to be stable. When the stress ratio was less than 0.55, the creep strain was within 1%; When the creep strain was 0.8, the creep strain increased slightly, within 5%. It can be seen that the thermal creep deformation of Q460GJ steel was not significant when the temperature was less than 500 °C and the stress ratio is less than 0.8. As shown in Figure 6 (b) , (d) and (e), the thermal creep strain-time curves showed the first and second creep stages when the stress ratios were 0.3 and 0.55, but showed the second and third creep stages when the stress ratios were 0.8. When the stress ratio was less than or equal to 0.55, the creep strain was about 5%. The thermal creep strain-time curves of 12 mm Q460GJ plate specimens at 600 °C are shown in Figure 5 (f) and were almost the same with that of 8 mm thickness Q460GJ steel plate specimens. As shown in Figure 6 (g) and (i), the creep strain-time curves showed the first and second creep stages when the stress ratios were 0.2 and 0.3, but showed the second and third creep stages when the stress ratios were 0.55. When the stress ratio was less than or equal to 0.3, the creep strain was about 20%. Under the stress ratio of 0.55, the failure of the specimens occurred at about 200 minutes. The thermal creep strain-time curves were almost the same with that of 8 mm thickness Q460GJ steel plate specimens. The thermal creep strain-time curves of 12 mm Q460GJ plate specimens at 700 °C and 800 °C are shown in Figure 6 (h) and (j) and were almost the same with that of 8 mm thickness Q460GJ steel plate specimens.

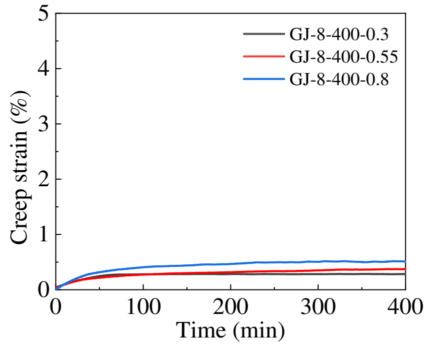

(a) 8 mm Q460GJ plate specimens at 400 °C

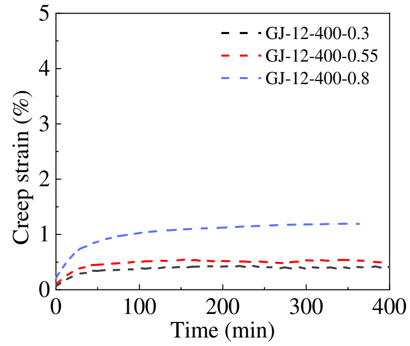

(b) 12 mm Q460GJ plate specimens at 400 °C

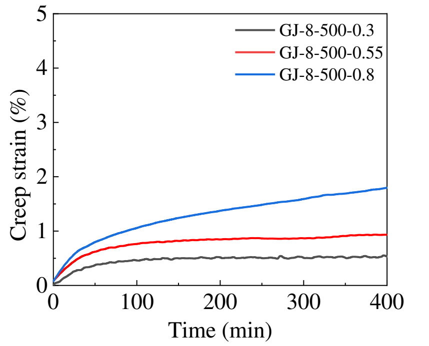

(c) 8 mm Q460GJ plate specimens at 500 °C

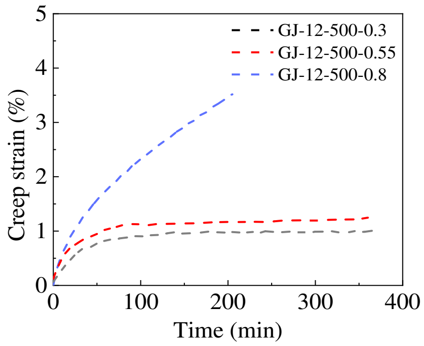

(d) 12 mm Q460GJ plate specimens at 500 °C

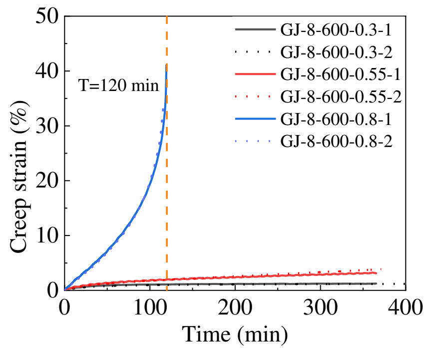

(e) 8 mm Q460GJ plate specimens at 600 °C

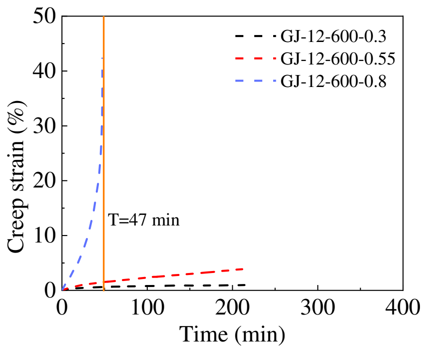

(f) 12 mm Q460GJ plate specimens at 600 °C

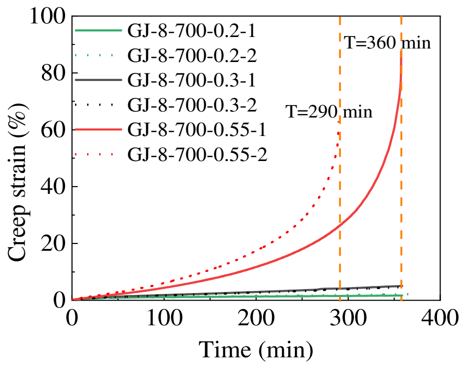

(g) 8 mm Q460GJ plate specimens at 700 °C

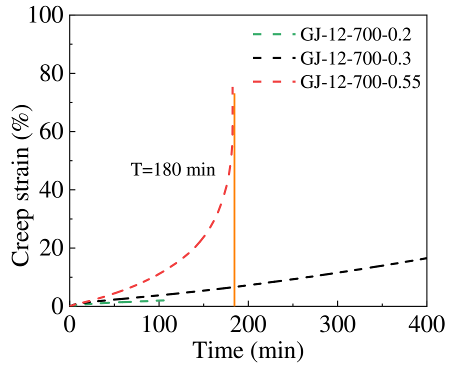

(h) 12 mm Q460GJ plate specimens at 700 °C

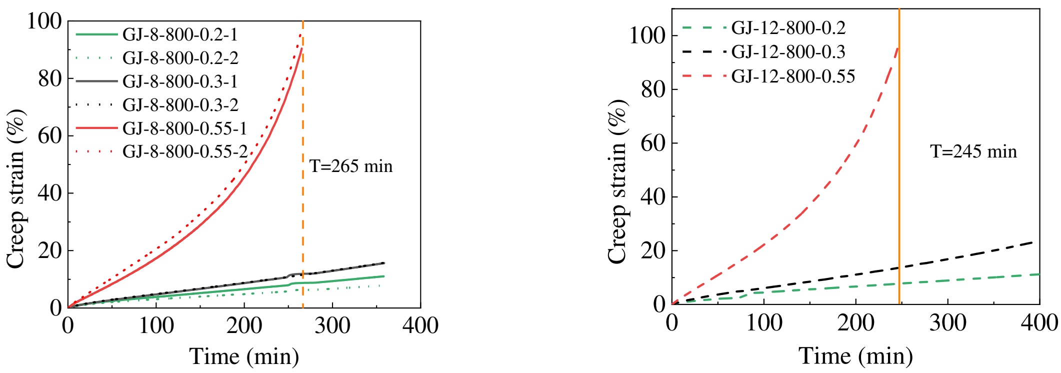

(i) 8 mm Q460GJ plate specimens at 800 °C (j) 12 mm Q460GJ plate specimens at 800 °C

Fig. 6. Thermal creep strain-time curves of Q460GJ steel specimens at different temperatures.

Generally, the thermal creep strain-time curves of two specimens under the same testing conditions were very close as shown in Figure 6 (e), (g) and (i), and there was partial deviation under high stress ratio, but the creep trend was basically the same. These phenomena are basically consistent with the description as reference [19] indicated. It can also be concluded that the thickness effect could be negligible for Q460GJ steel plates with thicknesses of 8 mm and 12 mm. The typical thermal creep strain-time curve of Q460GJ steel includes the typical three stages (the instantaneous creep stage, the steady-state creep stage and the accelerated creep stage) before fracture. The thermal creep strain increases with the increases of temperature and stress ratio.

4.3 Thermal creep rate curves

The thermal creep rate in the steady-state creep stage, the second stage creep rate, is an important parameter to investigate the thermal creep performance of steel. According to the thermal creep strain-time curves, the thermal creep rate curves of Q460GJ steel at different temperatures are shown in Figure 7-11. The thermal creep rate curves and creep stage demarcation at of 8 mm and 12 mm Q460GJ plate specimens at 400 °C are shown in Figure 7. All creep rate curves include transient creep stage (I) and steady-state creep stage (II). At 400 °C, the creep stage demarcation times were about 65 min. The thermal creep rate curves and creep stage demarcation at of 8 mm and 12 mm Q460GJ plate specimens at 500 °C are shown in Figure 8. All creep rate curves include transient creep stage (I) and steady-state creep stage (II). At 500 °C, the creep stage demarcation times of stage (I) and (II) were about 70 min.

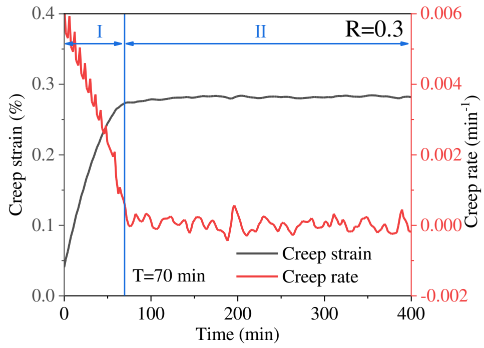

(a) 8mm, R=0.3

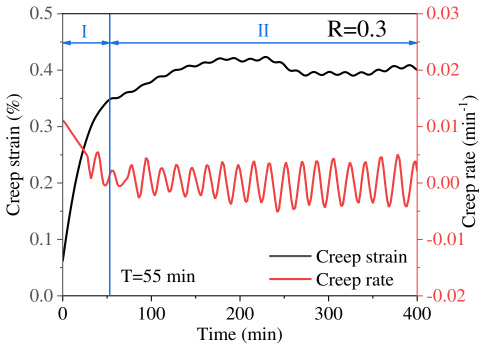

(b) 12mm, R=0.3

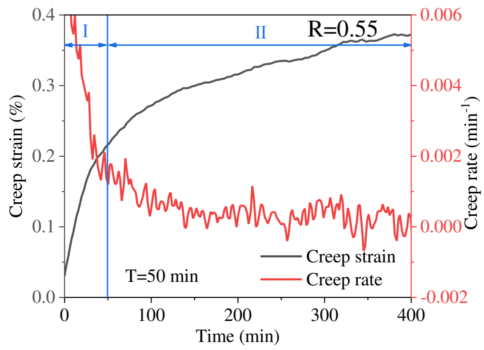

(c) 8mm, R=0.55

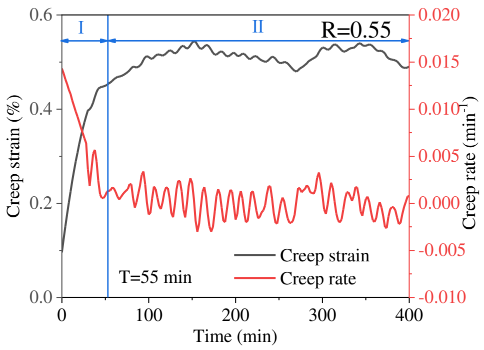

(d) 12mm, R=0.55

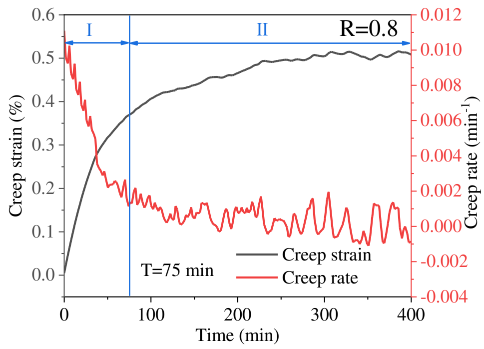

(e) 8mm, R=0.8

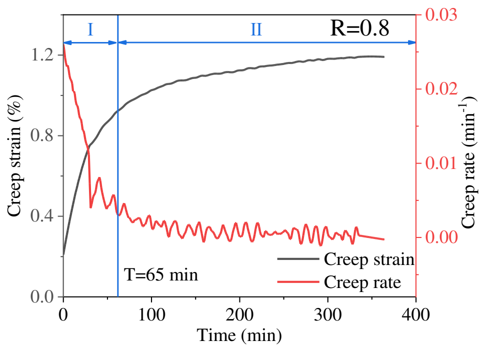

(f) 12mm, R=0.8

Fig. 7. Thermal creep strain rate curves and creep stage demarcation at 400 °C.

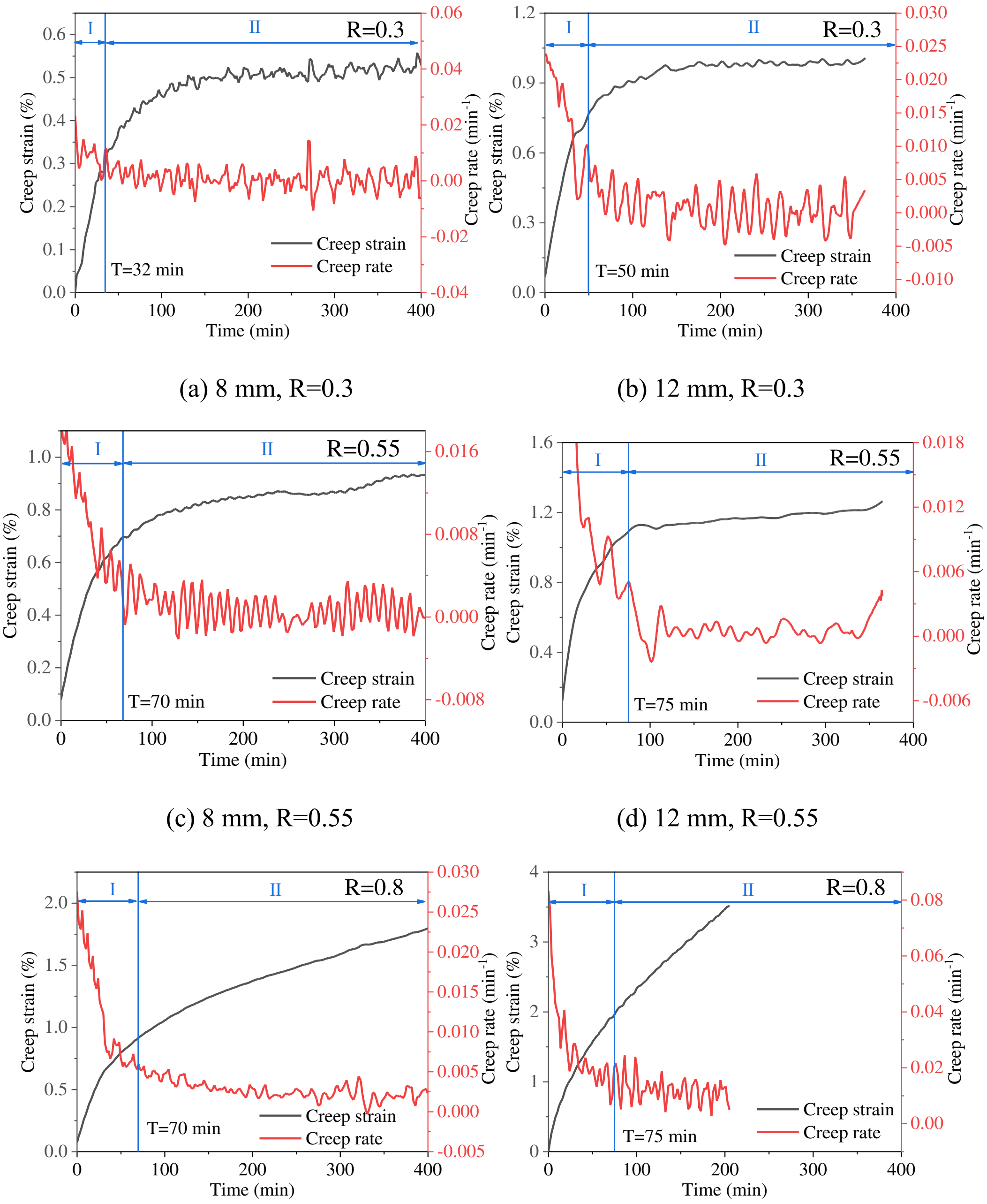

(a) 8 mm, R=0.3 (b) 12 mm, R=0.3

(c) 8 mm, R=0.55 (d) 12 mm, R=0.55

(e) 8 mm, R=0.8 (f) 12 mm, R=0.8

Fig. 8. Thermal creep strain rate curves and creep stage demarcation at 500 °C.

The thermal creep rate curves and creep stage demarcation at of 8 mm and 12 mm Q460GJ plate specimens at 600 °C are shown in Figure 9. When the stress ratios are 0.3 and 0.55, the creep rate curves include transient creep stage (I) and steady-state creep stage (II). When the stress ratio is 0.8, the creep rate curves include transient creep stage (I), steady-state creep stage (II) and the accelerated creep stage (III). At 600 °C, the creep stage demarcation times of stage (I) and (II) were about 30 min.

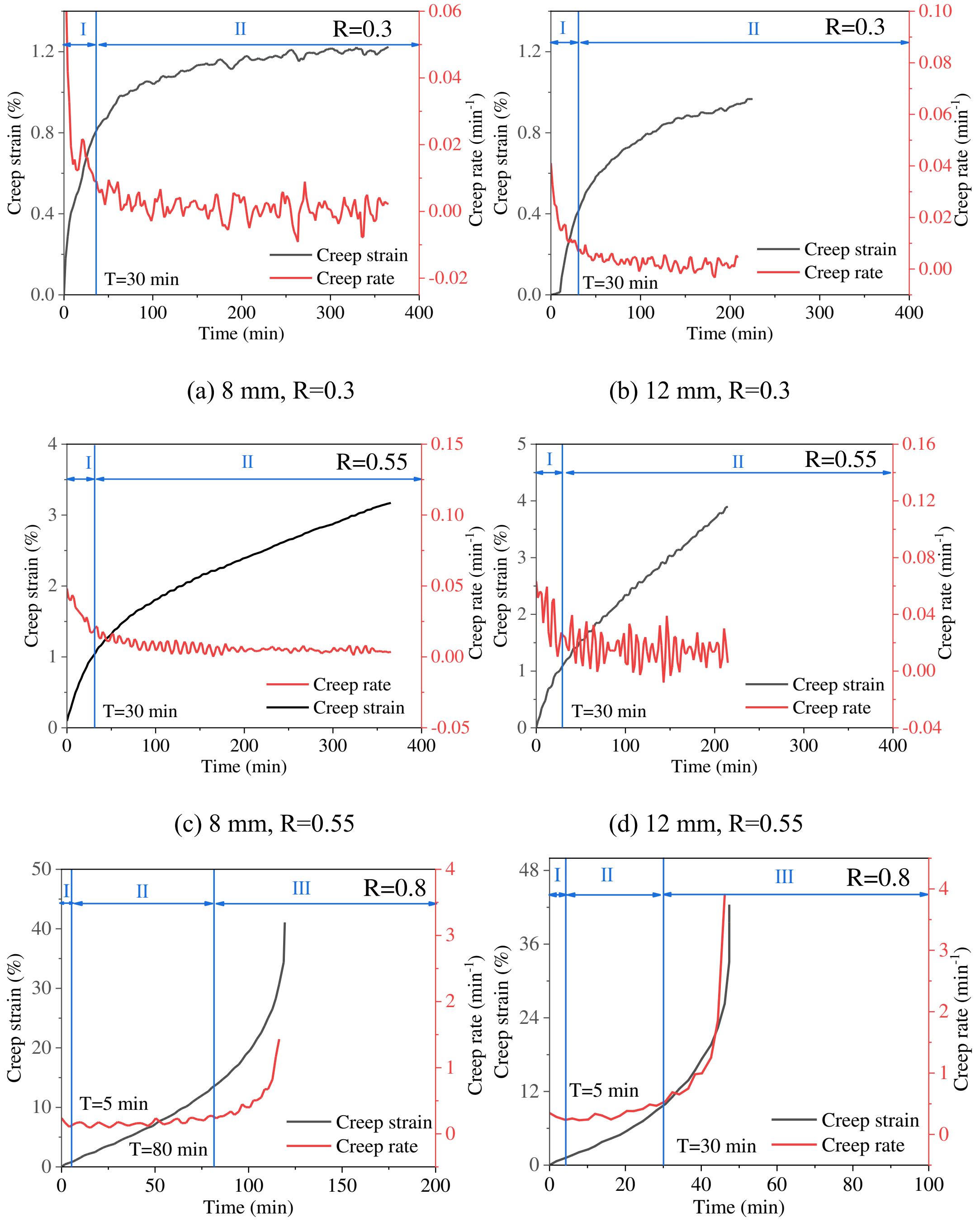

(a) 8 mm, R=0.3 (b) 12 mm, R=0.3

(c) 8 mm, R=0.55 (d) 12 mm, R=0.55

(e) 8 mm, R=0.8 (f) 12 mm, R=0.8

Fig. 9. Thermal creep strain rate curves and creep stage demarcation at 600 ºC.

The thermal creep rate curves and creep stage demarcation at of 8 mm and 12 mm Q460GJ plate specimens at 700 ºC are shown in Figure 10. When the stress ratios are 0.2 and 0.3, the creep rate curves include transient creep stage (I) and steady-state creep stage (II). When the stress ratio is 0.55 and 0.8, the creep rate curves include transient creep stage (I), steady-state creep stage (II) and the accelerated creep stage (III). At 700 ºC, the creep stage demarcation times of stage (I) and (II) were about 20 min.

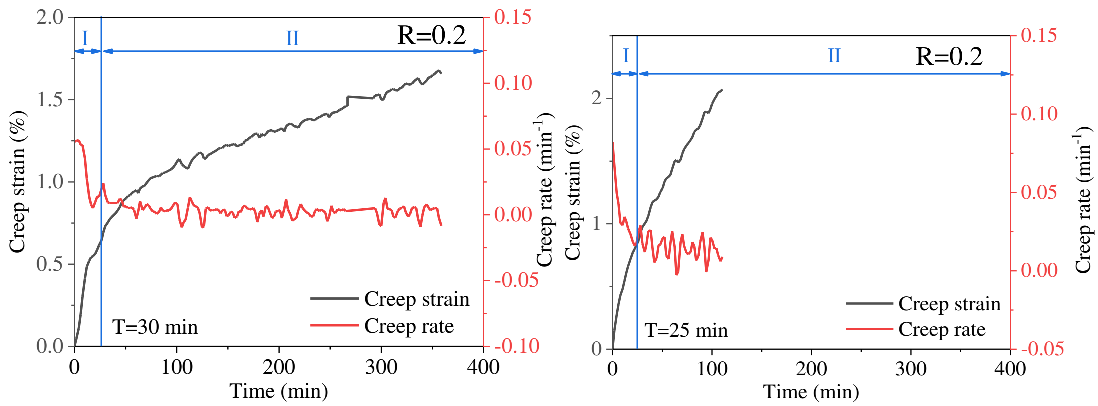

(a) 8 mm, R=0.2 (b) 12 mm, R=0.2

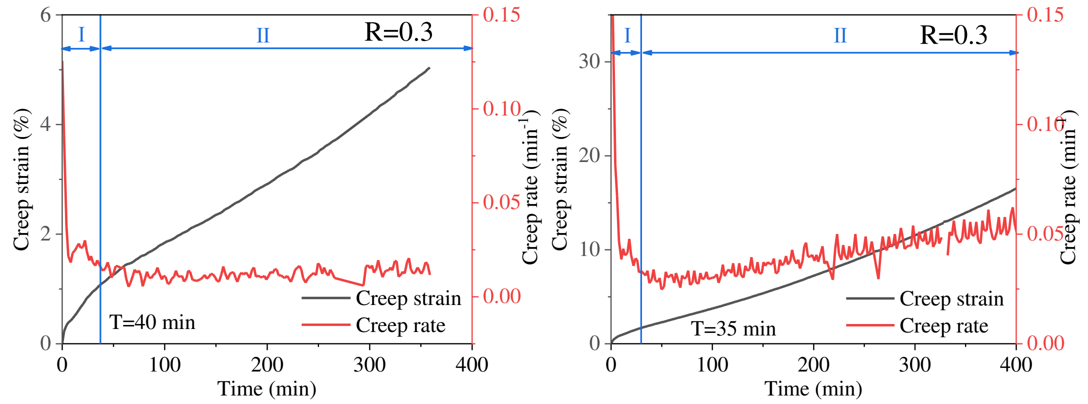

(c) 8 mm, R=0.3 (d) 12 mm, R=0.3

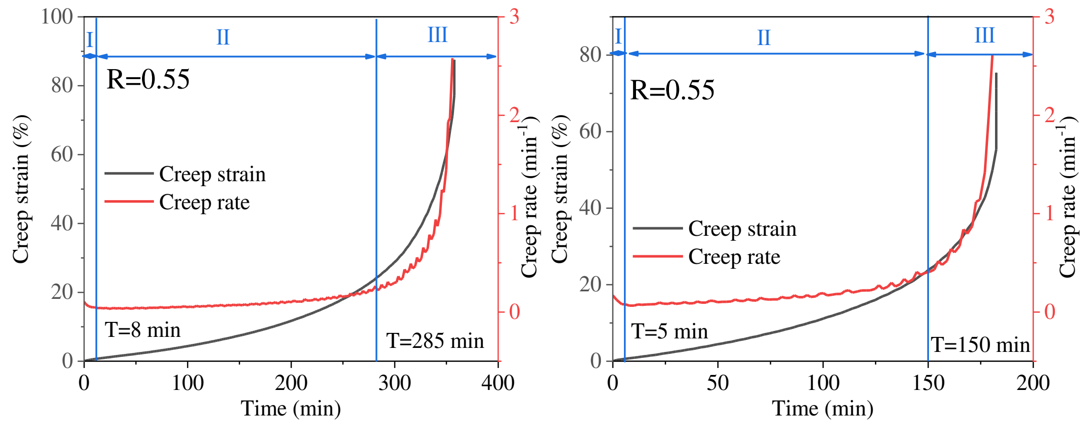

(e) 8 mm, R=0.55 (f) 12 mm, R=0.55

Fig. 10. Thermal creep strain rate curves and creep stage demarcation at 700 ºC.

The thermal creep rate curves and creep stage demarcation at of 8 mm and 12 mm Q460GJ plate specimens at 800 ºC are shown in Figure 11. When the stress ratios are 0.2 and 0.3, the creep rate curves include transient creep stage (I) and steady-state creep stage (II). When the stress ratio is 0.55 and 0.8, the creep rate curves include transient creep stage (I), steady-state creep stage (II) and the accelerated creep stage (III). At 800 ºC, the creep stage demarcation times of stage (I) and (II) were about 20 min.

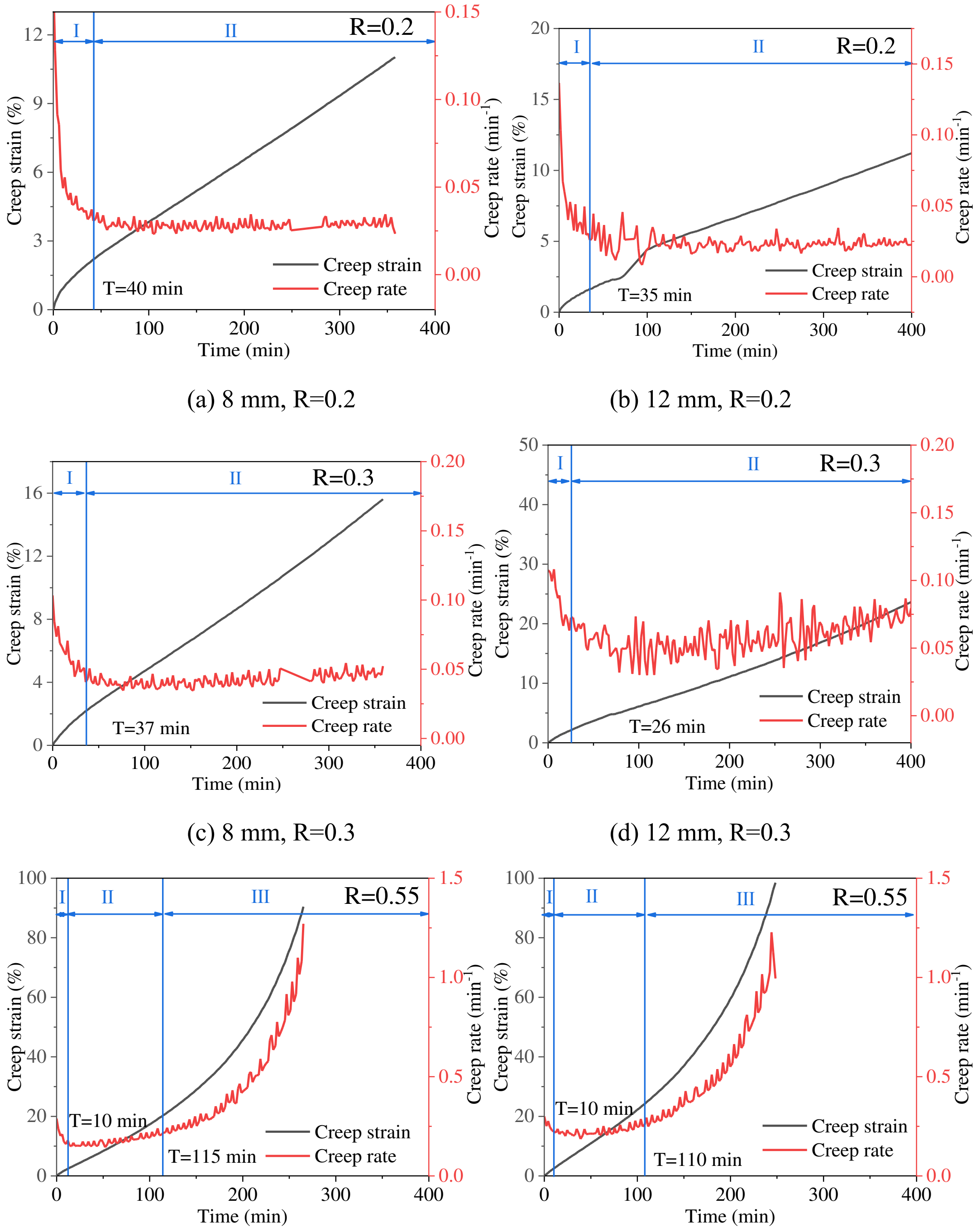

(a) 8 mm, R=0.2 (b) 12 mm, R=0.2

(c) 8 mm, R=0.3 (d) 12 mm, R=0.3

(e) 8 mm, R=0.55 (f) 12 mm, R=0.55

Fig. 11. Thermal creep strain rate curves and creep stage demarcation at 800 °C.

It can be found that the third stage of thermal creep strain-time curve will appear rapidly when the temperature and stress ratio are higher. For 12 mm thickness Q460GJ steel plate, the thermal creep rate curves observed from creep tests were almost the same with that of 8 mm thickness Q460GJ steel plate specimens. There was no obvious thickness effect observed for Q460GJ steel plates with thicknesses of 8 mm and 12 mm.

By selecting the thermal creep strain rate data of steady-state creep stage for linear fitting, the slope of the fitting line was the chosen as the average value of the second stage creep strain rate. The second stage creep strain rates of 8 mm Q460GJ steel at elevated temperatures (min^{-1}) are shown in Table 4. The second stage creep strain rates of 12 mm Q460GJ steel at elevated temperatures (min^{-1}) are shown in Table 5. Under the same stress ratio, the thermal creep strain rate increases with the increase of temperature. At the same temperature, the thermal creep strain rate increases with the increase of stress ratio. There was little difference between the thermal creep strain rate values of 8 mm Q460GJ steel and 12 mm Q460GJ steel at elevated temperatures within 600 ºC. It can be found that the thermal creep strain rate at each stress ratio is relatively small within 500 ºC. When the stress ratio is above 0.3 and the temperature is above 700 ºC, the thermal creep strain rate increases rapidly. The temperature and stress ratio have a great influence on the thermal creep strain rate of Q460GJ steel. Within the testing conditions set in this paper, the variation range of the thermal creep strain rate is 3.07E-05 (min^{-1}) to 0.288 (min^{-1}). The loading accuracy of the instrument in this article was 0.5 %. When the strain is small, as shown in Figure 8-11, there are some oscillations of the experimental results. The oscillations of the experimental results were relatively obvious. This might be caused by loading fluctuations. Based on the thermal creep strain time curves, thermal creep strain rate curves and creep stage degradation, the difference for thickness influence on thermal creep property could be ignored, this might be caused by the less than 5% difference for thickness influence on thermal mechanical property [29].

Table 4 The second stage creep strain rate of 8mm Q460GJ steel at elevated temperatures (min^{-1}).

Stress ratio R	400 °C	500 °C	600 °C	700 °C	800 °C
0.2	-	-	-	2.15E-03	2.83E-02
0.3	3.54E-04	2.13E-04	7.18E-04	1.23E-02	4.29E-02
0.55	3.43E-04	5.64E-04	5.24E-03	8.04E-02	0.177
0.8	3.54E-04	2.26E-03	0.164	-	-

Table 5 The second stage creep strain rate of 12mm Q460GJ steel at elevated temperatures (min^{-1}).

Stress ratio R	400 °C	500 °C	600 °C	700 °C	800 °C
0.2	-	-	-	1.40E-02	2.31E-02
0.3	3.07E-05	3.92E-04	2.24E-03	5.17E-02	5.94E-02
0.55	1.77E-04	3.51E-04	1.49E-02	0.141	0.226
0.8	6.26E-04	1.14E-02	0.288	-	-

5. Discussion on thermal creep of Q460GJ and Q460 steel

The thermal creep test results of Q460GJ steel in this paper were compared with those of Q460 high-strength steel in reference [30] The thermal creep strain-time curves comparisons of Q460GJ steel and Q460 steel are shown in Figure 12. Figure 12(a) shows the creep strain-time curves of Q460GJ steel and Q460 steel at 400 °C. While the stress levels were close, the second stage creep strain rates of Q460GJ steel were lower than that of Q460 steel. Figure 12 (b) and (c) show the creep strain-time curves of Q460GJ steel and Q460 steel at 500 °C and 600 °C. While the stress levels were close, the second stage creep strain rates of Q460 steel were obviously higher than that of Q460GJ steel. Figure 12 (d) and (e) show the creep strain-time curves of Q460GJ steel and Q460 steel at 700 °C and 800 °C. While the stress levels were close, there were no obvious difference between the second stage creep strain rates of Q460 steel and Q460GJ steel. Generally, the thermal creep strain-time curves of the two kinds of steels were similar, the creep strain increased with the increase of temperature, and the order of magnitude of the creep strain was basically the same. When the temperature was no more than 600 °C, the second stage creep strain rates of Q460 steel were obviously higher than that of Q460GJ steel while the stress levels were close. At 700 °C and 800 °C, there were no obvious difference between the second stage creep strain rates of Q460 steel and Q460GJ steel while the stress levels were close. Under the same conditions, the second stage creep strain rates of Q460GJ steel were obviously lower than that of Q460 steel, and it will be safer for Q460GJ steel structure under elevated temperatures within 600 °C than Q460 steel.

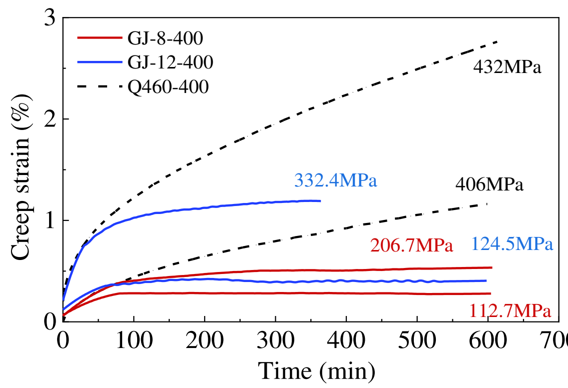

(a) Creep strain-time curves at 400 °C

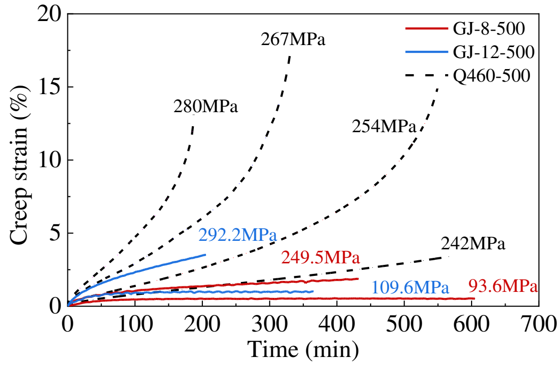

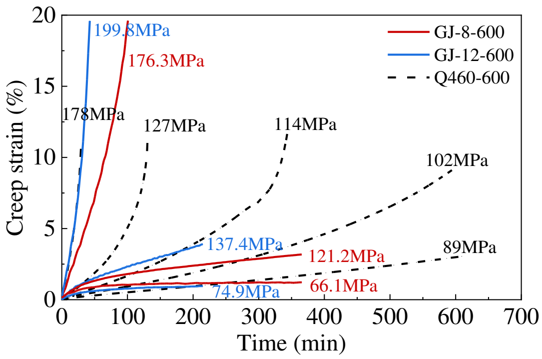

(b) Creep strain-time curves at 500 °C (c) Creep strain-time curves at 600 °C

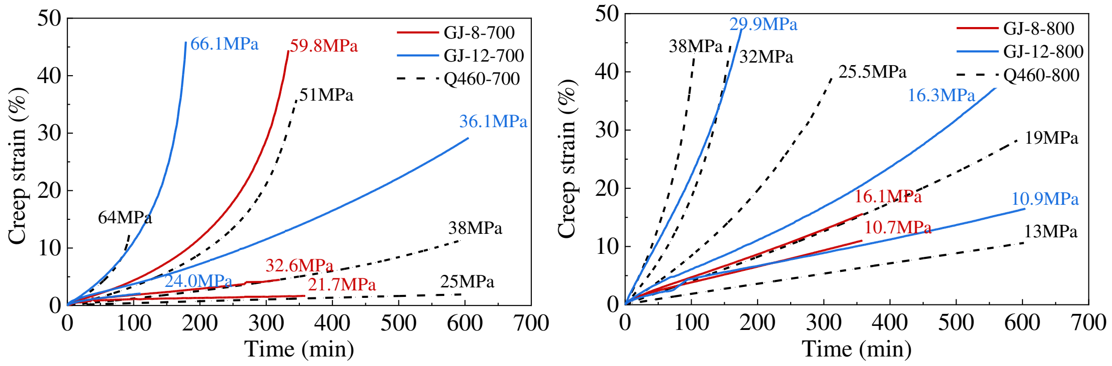

(d) Creep strain-time curves at 700 °C (e) Creep strain-time curves at 800 °C

Fig. 12. Thermal creep strain-time curves comparison of Q460GJ steel and Q460 steel.

6. Thermal creep strain-time curve model

In order to describe the thermal creep behavior of materials, a lot of research on creep constitutive model has been carried out. Many scholars have established different creep constitutive models based on the creep tensile test results. The most commonly used creep models are Harmathy model [34], Fields & Fields model [35] and Kodur model [36]. In this paper, the Fields & Fields creep model is used, which gives the relationship between creep strain, time and stress in power function form as shown in equation (1). The Fields & Fields creep model widely used in fire engineering is concise and has few parameters. The model can be directly applied to the finite element software ABAQUS analysis after first-order derivation. The creep rate ($d\varepsilon/dt$) can be calculated as equation (2).

$$\varepsilon^{cr} = at^{b}\sigma^{c} \tag{1}$$

where ε^{cr} is the creep strain (%), t is the time (min), σ is the stress (MPa), a and b are dimensionless parameters.

$$d\varepsilon / dt = abt^{b-1}\sigma^{c} \tag{2}$$

where $d\varepsilon/dt$ is the creep rate (% / min).

The Fields & Fields creep model fitting results for Q460GJ steel creep strain-time curves are shown in Figure 13. At 400 °C, it can be seen that when the applied stress increased from 113 MPa to 332.4 MPa, the creep strain increased with the increase of stress, and the fitting degree of the Fields & Fields creep was good. At 500 °C, it can be seen that when the applied stress increased from 93.6 MPa to 292 MPa, the creep strain increased with the increase of stress, and the fitting degree of the Fields & Fields creep was good. At 600 °C, it can be seen that when the applied stress increased from 66.1 MPa to 199.8 MPa, the creep strain increased with the increase of stress, and the fitting degree of the Fields & Fields creep was good. At 700 °C, it can be seen that when the applied stress increased from 21.7 MPa to 66.1 MPa, the creep strain increased with the increase of stress, and the fitting degree of the Fields & Fields creep was good. At 800 °C, it can be seen that when the applied stress increased from 10.7 MPa to 29.9 MPa, the creep strain increased with the increase of stress, and the fitting degree of the Fields & Fields creep was good. The parameters of the Fields & Fields creep model fitting for Q460GJ steel are shown in Table 6. The statistical mean absolute errors between the experimental curves and model curves under different temperatures were calculated as shown in Table 6. The model formulations fit slightly poorly for low temperature creep test results, but fit well for high temperature creep test. At temperatures of 400 °C and 500 °C, the effectiveness of the model simulation is slightly lower, which may be due to the relatively smaller creep deformation. The relationship between temperatures (T) and the parameters of the Fields & Fields creep model fitting for Q460GJ steel are shown as equations (3-5). To sum up, The Fields & Fields creep model is suitable for fitting the thermal creep strain-time curves for Q460GJ steel, and equations (3-5) can be used to calculate the model parameters at different temperatures.

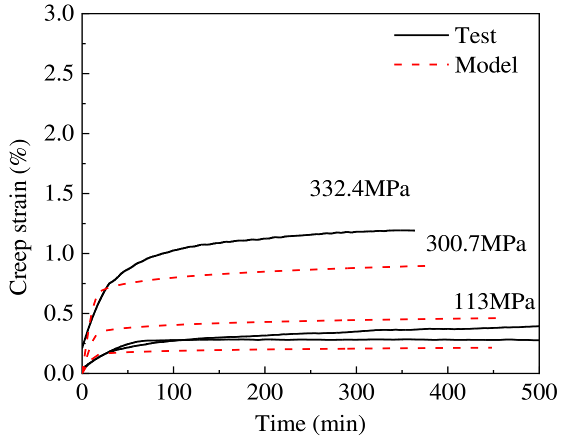

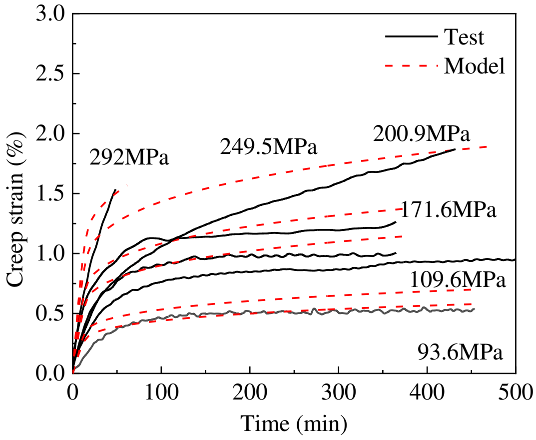

(a) Fields & Fields creep model at 400 °C (b) Fields & Fields creep model at 500 °C

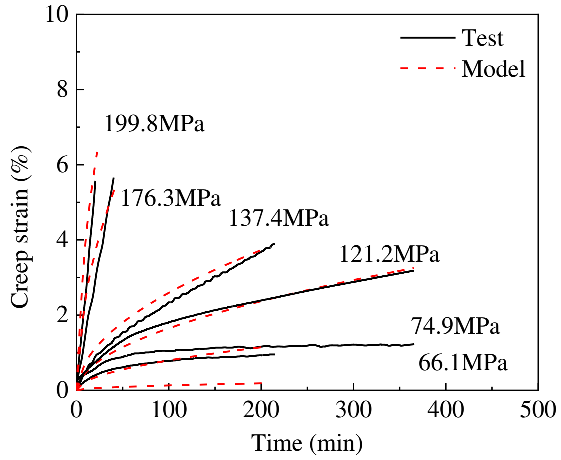

(c) Fields & Fields creep model at 600 °C

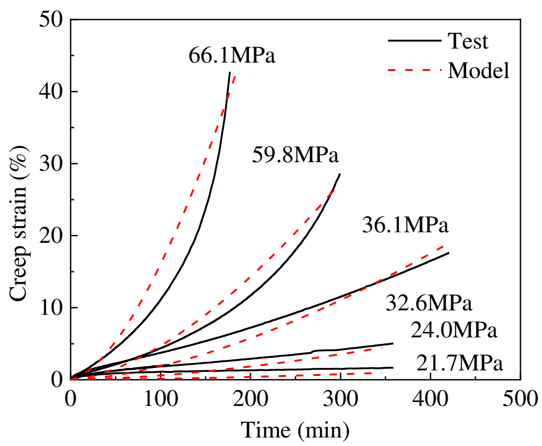

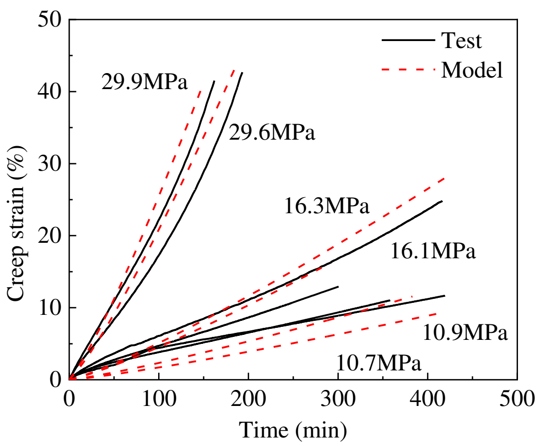

(d) Fields & Fields creep model at 700 °C (e) Fields & Fields creep model at 800 °C

Fig. 13. The Fields & Fields creep model fittings for Q460GJ steel creep strain-time curves

Table 6 Parameters of the Fields & Fields creep model fitting for Q460GJ steel

Temperature (°C)	*a*	log(*a*)	*b*	*c*	COD(R^2)	Mean Absolute Error (%)
400	3.31E-04	-3.48	0.87	1.26	0.975	0.073
500	8.64E-04	-3.06	0.18	1.19	0.986	0.076
600	2.34E-10	-9.63	0.52	4.23	0.998	0.240
700	6.22E-11	-10.21	1.60	4.49	0.994	0.683
800	6.80E-06	-5.17	1.19	2.86	0.992	0.867

$$\log(a)=\begin{cases} -2.500\times10^{-5}T^2-7.400\times10^{-4}T+0.873 & 400℃\le T\le 700℃ \\ -5.170 & 700℃< T\le 800℃ \end{cases} \quad (3)$$

$$b=\begin{cases} 4.420\times10^{-5}T^2-0.046T+12.233 & 400℃\le T\le 700℃ \\ 1.190 & 700℃< T\le 800℃ \end{cases} \quad (4)$$

$$c=\begin{cases} 8.250\times10^{-6}T^2+0.003T-1.816 & 400℃\le T\le 700℃ \\ 2.860 & 700℃< T\le 800℃ \end{cases} \quad (5)$$

7. Conclusions

The present study was designed to study the creep properties of Q460GJ steel at elevated temperatures. The thermal creep strain-time curves of Q460GJ steel were compared with that of Q460 steel and analyzed. The Fields & Fields model was selected to fit the thermal creep strain-time curves of Q460GJ steel at elevated temperatures, and the creep characteristics of Q460GJ steel were comprehensively characterized. Based on the above works, the following major findings were revealed.

(1) When the temperature exceeds about 500 °C and the stress ratio is greater than about 0.55, the Q460GJ steel plate specimens have obvious creep deformations, so it is

necessary to consider the thermal creep deformation of steel at elevated temperatures for steel structural design. Generally, for Q460GJ and Q460 steels, the creep strain increased with the increase of temperature, and the order of magnitude of the creep strain was basically the same. The difference in plate thickness does not affect the creep properties of the 8 mm and 12 mm Q460GJ steel plates at elevated temperatures.

(2) The typical high temperature creep stress-train curve of Q460GJ steel includes the typical three stages before fracture. The thermal creep strain increases with the increases of temperature and stress ratio. Under the same test conditions, the thermal creep strain rates of Q460GJ steel were obviously lower than that of Q460 steel, and it will be safer for Q460GJ steel structure under elevated temperatures within 600 ºC than Q460 steel. At 700 ºC and 800 ºC, there were no obvious difference between the second stage creep strain rates of Q460 steel and Q460GJ steel while the stress levels were close.

(3) The creep strain rate at each stress ratio is relatively small within 500 ºC. When the stress ratio is above 0.3 and the temperature is above 700 ºC, the creep strain rate increases rapidly. The temperature and stress ratio have a great influence on the thermal creep strain rate of Q460GJ steel. Within the testing conditions set in this paper, the variation range of the thermal creep strain rate is 3.07E-05 (min^{-1}) to 0.288 (min^{-1}).

(4) The Fields & Fields creep model is suitable for fitting the thermal creep strain-time curves for Q460GJ steel by using the proposed parameters at different temperatures. Further revealing the influence of the microstructure and composition of the Q460GJ steel on the thermal creep properties is the further recommended work that

is ongoing to be carried out.

Acknowledgment

The authors wish to acknowledge the support of the Natural Science Foundation of Chongqing (cstc2021jcyj-jqX0021). Any opinions, findings, conclusions, or recommendations expressed in this paper are those of the authors and do not necessarily reflect the views of the sponsors.

References

[1] Bjorhovde R. Development and use of high performance steel[J]. Journal of Constructional Steel Research, 2004, 60(3-5): 393-400.

[2] Wang W, Li S, Ran T. Numerical Study on High Strength Q690 Steel Flush End-Plate Connections at Elevated Temperatures[J]. Fire Technology, 2024: 1-26.

[3] Yun X, Wang Z, Gardner L. Full-range stress–strain curves for aluminum alloys[J]. Journal of Structural Engineering, 2021, 147(6): 04021060.

[4] Yu Y, Lan L, Ding F, et al. Mechanical properties of hot-rolled and cold-formed steels after exposure to elevated temperature: A review[J]. Construction and Building Materials, 2019, 213: 360-376.

[5] GB/T 19879, Steel plates for building structures, Standards Press of China, Beijing, 2023 (in Chinese).

[6] Kodur V K, Aziz E M. Effect of temperature on creep in ASTM A572 high-strength low-alloy steels[J]. Materials and Structures, 2015, 48: 1669-1677.

[7] Hantouche E G, Al Khatib K K, Morovat M A. Modeling creep of steel under transient temperature conditions of fire[J]. Fire Safety Journal, 2018, 100: 67-75.

[8] Wang W, Yan S, Kodur V. Temperature induced creep in low-alloy structural Q345 steel[J]. Journal of Materials in Civil Engineering, 2016, 28(6): 06016003.

[9] Morovat M, Engelhardt M, Helwig T, et al. High-temperature creep buckling phenomenon of

steel columns subjected to fire[J]. Journal of Structural Fire Engineering, 2014, 5(3): 189-202.

[10] Li G Q, Zhang C. Creep effect on buckling of axially restrained steel columns in real fires[J]. Journal of Constructional Steel Research, 2012, 71: 182-188.

[11] Wu Z, Li L, Wu R, et al. Determination of high-temperature creep and post-creep response of structural steels[J]. Journal of Constructional Steel Research, 2022, 193: 107287.

[12] Kodur V K R, Dwaikat M M S. Effect of high temperature creep on the fire response of restrained steel beams[J]. Materials and Structures, 2010, 43: 1327-1341.

[13] Torić N, Harapin A, Boko I. Experimental verification of a newly developed implicit creep model for steel structures exposed to fire[J]. Engineering Structures, 2013, 57: 116-124.

[14] Huang Z F, Tan K H, Ting S K. Heating rate and boundary restraint effects on fire resistance of steel columns with creep[J]. Engineering Structures, 2006, 28(6): 805-817.

[15] Zhou X, Yang J, Wang W, et al. Mechanical properties and creep strain of Q355 cold-formed steel at elevated temperature[J]. Journal of Constructional Steel Research, 2021, 180: 106577.

[16] Brnic J, Canadija M, Turkalj G, et al. Behaviour of S 355JO steel subjected to uniaxial stress at lowered and elevated temperatures and creep[J]. Bulletin of Materials Science, 2010, 33: 475-481.

[17] Wang W, Wang K, Kodur V, et al. Mechanical properties of high-strength Q690 steel at elevated temperature[J]. Journal of Materials in Civil Engineering, 2018, 30(5): 04018062.

[18] Wang W, Zhang Y, Xu L, et al. Mechanical properties of high-strength Q960 steel at elevated temperature[J]. Fire Safety Journal, 2020, 114: 103010.

[19] Li G Q, Wang X X, Zhang C, et al. Creep behavior and model of high-strength steels over 500 MPa at elevated temperatures[J]. Journal of Constructional Steel Research, 2020, 168: 105989.

[20] Brnic J, Turkalj G, Canadija M, et al. Creep behavior of high-strength low-alloy steel at elevated temperatures[J]. Materials Science and Engineering: A, 2009, 499(1-2): 23-27.

[21] Craveiro H D, Rodrigues J P C, Santiago A, et al. Review of the high temperature mechanical and thermal properties of the steels used in cold formed steel structures–The case of the S280 Gd+ Z steel[J]. Thin-Walled Structures, 2016, 98: 154-168.

[22] Huang D, Kodur V, Wang W. Temperature-dependent properties of high-strength steel for evaluating the fire resistance of structures[J]. Advances in Structural Engineering, 2023, 26(12): 2265-2281.

[23] Qiang X, Bijlaard F S K, Kolstein H. Elevated-temperature mechanical properties of high strength structural steel S460N: Experimental study and recommendations for fire-resistance design[J]. Fire Safety Journal, 2013, 55: 15-21.

[24] Al-azzani H, Yang J, Sharhan A, et al. A practical approach for fire resistance design of restrained high-strength Q690 steel beam considering creep effect[J]. Fire Technology, 2021, 57: 1683-1706.

[25] El Ghor A H, Hantouche E G. Thermal creep mechanical-based modeling for flush endplate connections in fire[J]. Journal of Constructional Steel Research, 2017, 136: 11-23.

[26] Jabotian H V, Hantouche E G. Thermal creep behavior of shear tabs in fire using modified burgers model[J]. Journal of Constructional Steel Research, 2019, 160: 528-539.

[27] Venkatachari S, Kodur V K R. Effect of transient creep on fire induced instability in steel framed structures[J]. Journal of Constructional Steel Research, 2021, 181: 106618.

[28] Wu Z, Liu Z, Li L, et al. Experimental and neural networks analysis on elevated-temperature mechanical properties of structural steels[J]. Materials Today Communications, 2022, 32: 104092.

[29] Li S, Li A, Wang W. Mechanical properties and constitutive models of Q460GJ steel at elevated temperatures [J]. Journal of Constructional Steel Research, 221 (2024): 108924.

[30] Wang W, Yan S, Liu J. Studies on temperature induced creep in high strength Q460 steel [J]. Materials and Structures, 2017, 50: 1-14.

[31] CECS200:2006, Chinese Technical Code for Fire Safety of Steel Structure in Buildings, China Plan Press, 2006. (in Chinese).

[32] GB/T 2039-2012, Metallic Materials-uniaxial Creep Testing Method in Tension, Standards Press of China, Beijing, China, 2012 (in Chinese).

[33] GB/T 228, 2 Metallic Materials-Tensile Testing Part 2: Method of Test at Elevated Temperature, Standards Press of China, Beijing, 2015 (in Chinese).

[34] Harmathy T Z . A comprehensive creep model [J]. Journal of Basic Engineering, 1967, 89(2).

[35] Fields B A, Fields R J. Elevated temperature deformation of structural steel [M]. National Institute of Standards and Technology, Gaithersburg, 1989.

[36] Kodur V K R, Dwaikat M M S. Effect of high temperature creep on the fire response of restrained steel beams[J]. Materials and Structures, 2010,43(10):1327-1341.